Visualization of epithelial cell adhesion molecule-expressing renal cell carcinoma xenografts using designed ankyrin repeat protein Ec1 labelled with ^{99m}Tc and ^{125}I

VLADIMIR TOLMACHEV[1,2], VITALINA BODENKO[2,3], ANNA ORLOVA[2,4], ALEXEY SCHULGA[2,5], SERGEY M. DEYEV[2,5] and ANZHELIKA VOROBYEVA[1]

[1]Department of Immunology, Genetics and Pathology, Uppsala University, 75185 Uppsala, Sweden; [2]Research Centrum for Oncotheranostics, Research School of Chemistry and Applied Biomedical Sciences, National Research Tomsk Polytechnic University; [3]Department of Pharmaceutical Analysis, Siberian State Medical University, 634050 Tomsk, Russia; [4]Department of Medicinal Chemistry, Uppsala University, 75105 Uppsala, Sweden; [5]Molecular Immunology Laboratory, Shemyakin and Ovchinnikov Institute of Bioorganic Chemistry, Russian Academy of Sciences, 117997 Moscow, Russia

Received July 18, 2022; Accepted October 5, 2022

DOI: 10.3892/ol.2022.13598

Abstract. The upregulation of epithelial cell adhesion molecule (EpCAM) expression, found in a substantial fraction of renal cell carcinomas (RCCs), renders it a potential molecular target for the treatment of disseminated RCC. However, the heterogeneous expression of EpCAM necessitates first identifying the patients with sufficiently high expression of EpCAM in tumors. Using the specific radionuclide-based visualization of EpCAM might enable such identification. The designed ankyrin repeat protein, Ec1, is a small (molecular weight, 18 kDa) targeting protein with a subnanomolar affinity to EpCAM. Using a modified Ec1, a tracer was developed for the radionuclide-based visualization of EpCAM *in vivo*, i.e., an EpCAM-visualizing designed ankyrin repeat protein (EVD). EVD was labelled with either technetium-99m using technetium tricarbonyl or with iodine-125 (as a surrogate for iodine-123) by coupling it to para-[^{125}I]iodobenzoyl ([^{125}I]PIB) groups. Both the ^{125}I-labelled EVD (^{125}I-EVD) and ^{99m}Tc-labelled EVD (^{99m}Tc-EVD) bound specifically to EpCAM-expressing SK-RC-52 renal carcinoma cells. The binding affinity (K_D value) of ^{99m}Tc-EVD to SK-RC-52 cells was 400±28 pM. The tracers' uptake in SK-RC-52 xenografts at 3 h after injection was 5.2±1.4%ID/g for ^{125}I-EVD and 6.0±1.4%ID/g for ^{99m}Tc-EVD (no significant difference). These uptake values in SK-RC-52 xenografts were significantly higher (P<0.001) than those in Ramos lymphoma xenografts (used as EpCAM-negative control). The tumor-to-blood uptake ratio was significantly higher for ^{99m}Tc-EVD (25±6) compared with that of ^{125}I-EVD (14±3). However, ^{125}I-EVD was associated with higher tumor-to-liver, tumor-to-salivary gland, tumor-to-spleen and tumor-to-intestinal wall ratios. This makes it the preferable tracer for visualizing EpCAM expression levels in the frequently occurring abdominal metastases of RCC.

Correspondence to: Professor Vladimir Tolmachev, Department of Immunology, Genetics and Pathology, Uppsala University, Dag Hammarskjölds väg 20, 75185 Uppsala, Sweden
E-mail: vladimir.tolmachev@igp.uu.se

Abbreviations: EpCAM, epithelial cell adhesion molecule; RCC, renal cell carcinoma; DARPin, designed ankyrin repeat protein; PIB, *para*-iodobenzoyl; pRCC, papillary RCC; cpRCC, chromophobe RCC; mAb, monoclonal antibody; EPR effect, enhanced permeability and retention effect; ESP, engineered scaffold protein; iTLC, instant thin-layer chromatography; PBS, 0.05 M phosphate-buffered saline, pH 7.5; PET, positron emission tomography; SPECT, single-photon emission computed tomography; $T_{1/2}$, half-life; HPEM, ((4-hydroxyphenyl)-ethyl)maleimide

Key words: RCC, EpCAM, radionuclide molecular imaging, SPECT, ^{125}I, ^{99m}Tc, DARPin Ec1, ESP

Introduction

Renal cell carcinoma (RCC) is the leading type of malignant tumor originating from the kidneys, and makes up about 90% of all malignant renal tumors (1). RCC develops from the epithelium of the proximal tubules and collecting ducts in the kidneys. According to the WHO classification, there are different subtypes of kidney carcinomas: clear cell, papillary, chromophobe and collecting duct carcinomas. The identification of renal cell carcinoma subtypes is essential in clinics, because RCC constitutes a heterogeneous group of tumors with prognostic uncertainty (2).

The incidence of RCC is increasing, and the treatment results remain unsatisfactory. Although patients with early disease can be treated with surgery at a high success rate, nearly 50% of RCC patients die within 5 years after being diagnosed (3). The decisive factor determining the clinical outcome is the development of distant metastases, and the 5-year survival rate of patients with metastatic lesions is less

than 10% (4). The use of non-targeted chemotherapy for the treatment of metastatic-RCC patients' is associated with indiscriminate toxicity (5). Currently, there is no chemotherapy for advanced kidney carcinoma providing high objective response rates. Chemotherapy in combination with cytokines (IFN-alpha and IL-2) or only cytokines have been studied, but this treatment is not effective and leads to additive toxicity (3). Due to the low efficiency of existing treatments, it is necessary to develop new approaches for both the therapy and diagnosis of renal cell carcinoma. Regarding new therapy approaches, some advances have been achieved by targeting either the vascular endothelial growth factor receptor or the mammalian target of rapamycin (5,6). Another promising treatment approach that has emerged, is the use of immune-checkpoint inhibitors (7). Still, there is an urgent need for the identification of new molecular targets and biomarkers, as well as the development of new targeted therapies for RCC (7).

One particularly promising molecular target for RCC is the epithelial cell adhesion molecule (EpCAM). EpCAM is highly expressed in multiple carcinoma types and promotes tumor proliferation. Importantly, EpCAM overexpression has been detected in a large fraction of RCC cases. There has also been a continuous development and evaluation of EpCAM-targeting therapeutics which include monoclonal antibodies or antibody fragments as well as their drug- and toxin-conjugates (8-12), the EpCAM-targeting trifunctional T-cell engaging antibody catumaxomab (Removab®) (13), targeted toxins based on scaffold proteins (14,15), and chimeric antigen receptor-modified T cells (16). Importantly, catumaxomab was successfully used in the treatment of malignant ascites which originated from EpCAM-positive renal cell carcinoma (17).

Clinical data suggests that EpCAM-targeted treatment is efficient in tumors with high target expression (18,19). However, the level of EpCAM expression is heterogeneous in RCC and it was found that the overexpression of EpCAM depends on the tumor cell histology. EpCAM expression was found in 36.3% of clear-cell RCC, in 81.3% of papillary RCC (pRCC) and in 78.3% of chromophobe RCC (cpRCC) (20). This heterogeneous expression of EpCAM in renal carcinoma is an essential problem for targeted-cancer therapy because it might cause an overtreatment. Consequently, patient stratification for therapy based on EpCAM expression in tumors is a high-priority task. Typically, target expression is determined by the immunohistochemical analysis of biopsy samples (18). The invasiveness of these procedures makes it difficult to perform multiple biopsies. This, in turn, prevents obtaining information about the heterogeneity of expression in different metastases or changes in expression that occur over time. The radionuclide-based molecular imaging of EpCAM expression is a promising alternative to biopsy-based methods.

The previously known approach to imaging molecular targets, which uses radiolabeled therapeutic monoclonal antibodies (mAbs), has several disadvantages (21-23). The large size of monoclonal antibodies (molecular weight of 150 kDa) causes a slow accumulation of the imaging probes in the tumor, along with a slow decrease of their concentration in the blood. Consequently, a reasonable imaging contrast might be achieved only four to seven days after injection. Another factor, which decreases the accuracy of imaging when using monoclonal antibodies, is the enhanced permeability and retention (EPR) effect, i.e., unspecific accumulation of macromolecules in tumors. This effect decreases the specificity of imaging (24). The use of engineered scaffold proteins (ESPs) as targeted probes in radionuclide diagnostics is a promising option (25). A comparison of several formats of targeting vectors suggests that imaging probes based on engineered scaffold proteins provide higher contrast than probes based on monoclonal antibodies or their derivatives (25). ESPs typically have high binding specificities and affinities to their selected therapeutic targets. In addition, their small size facilitates rapid localization in tumors and prompt excretion from the blood. These features provide a high contrast for imaging on the day of injection.

The structure of ESPs determines their affinity to molecular targets. Designed ankyrin repeat proteins (DARPins) are ESPs built from 4-6 blocks (each block containing 33 amino acids) with a total molecular weight of 14-18 kDa (26). Previous studies have shown that DARPin Ec1 binds to EpCAM with a very high affinity, 68 pM (27).

Selecting a strategy for the radiolabeling of ESPs requires special attention because these proteins are small (having molecular weights between 4 and 20 kDa), and therefore labeling could significantly change their physicochemical properties and affect their biodistribution pattern.

The aim of this study was to assess the potential of a DARPin Ec1 derivative, EpCAM-visualizing DARPin (EVD), for imaging EpCAM in an *in vivo* RCC model. A residualizing ^{99m}Tc-label and non-residualizing ^{125}I-label were evaluated for this purpose.

Materials and methods

Materials and instruments. Iodine-125 in the form of sodium iodide was provided by Perkin Elmer Sverige AB. Instant thin-layer chromatography (iTLC) on iTLC silica gel strips (Varian) was used for measurements of radiochemical yield and purity. A cyclone storage phosphor system (Packard Instrument Company) with the OptiQuant image analysis software (Perkin Elmer) was used for the quantitative assessment of iTLC. Cell-associated activity during *in vitro* studies and organ-associated activity in biodistribution evaluations were measured using an automated gamma-spectrometer (1480 Wizard). For animal studies, radioactivity was measured using an ionization chamber VDC-405 (Veenstra Instruments BV) for formulation of injected solutions. Cells were cultured in a humidified incubator with 5% CO_2 at 37˚C in RPMI medium (Biochrom) containing 10% fetal bovine serum (FBS) (Merck), 2 mM L-glutamine, 100 IU/ml penicillin and 100 μg/ml streptomycin (all from Biochrom).

Protein production and radiolabeling. The EpCAM-specific DARPin Ec1 was designed using the binding sequence published earlier (27). An amino acid sequence H-E-H-E-H-E ($(HE)_3$-tag) was introduced to the N-terminus of DARPin Ec1 for site-specific labelling using [^{99m}Tc]technetium tricarbonyl and to improve its biodistribution. The $(HE)_3$-containing Ec1 was designated as EpCAM-visualizing DARPin (EVD). The production of EVD has also been described previously (28). Mass-spectrometry analysis confirmed that the protein had the correct mass, which demonstrated its authenticity.

EVD was indirectly radioiodinated by using N-succinimidyl-para-(trimethylstannyl)benzoate as a precursor according to a previously published protocol (28,29). A stock solution of [^{125}I]iodide in 0.01 M NaOH (5-15 μl, 17-42 MBq) was added to 10 μl of 0.1% acetic acid in water. A solution of the precursor in 5% acetic acid in methanol (5 μl, 1 mg/ml) was added to this mixture followed by addition of chloramine-T (20 μg, 5 μl in water). The oxidative iododestannylation reaction was terminated after 5 min by the addition of sodium metabisulfite (30 μg, 5 μl in water). A solution of DARPin Ec1 (140 μg in a mixture of 40 μl of 0.05 M phosphate-buffered saline, pH 7.5, and 140 μl of 0.07 M borate buffer, pH 9.3) was added and the resulting solution was incubated at room temperature for 30 min. ^{125}I-EVD was purified using a NAP-5 column (Cytiva, Uppsala, Sweden) which was pre-equilibrated with 1% bovine serum albumin (BSA) in PBS and then eluted with PBS. A mixture of acetone:water (4:1) was used as the mobile phase for the development of iTLC strips to determine the radiochemical yield and radiochemical purity of ^{125}I-EVD.

Labelling of DARPin $(HE)_3$-Ec1 using [^{99m}Tc] $[Tc(CO)_3(H_2O)_3]^+$ was performed as described earlier (28,29). The eluate from a technetium generator (500 μl, 3 GBq of [^{99m}Tc] TcO_4^-) was added to a CRS kit. After the kit reconstitution, the solution was incubated at 100˚C for 30 min. After incubation, the solution containing [^{99m}Tc][$Tc(CO)_3(H_2O)_3]^+$ (12 μl) was mixed with a solution of EVD (40 μg) in 33 μl of PBS and incubated at 60˚C for 60 min. The radiolabeled DARPin EVD was purified using NAP-5 columns pre-equilibrated and eluted with PBS. PBS was used for the development of iTLC strips to determine the radiochemical yield and radiochemical purity of ^{99m}Tc-EVD.

Binding specificity and cellular processing assays. The EpCAM-expressing human renal cell carcinoma cell line SK-RC-52 (American Type Culture Collection) was used for *in vitro* studies. One day before the experiment, 1x10^6 cells per dish were seeded. Groups of three dishes were used per data point.

The evaluation of ^{125}I-EVD's and ^{99m}Tc-EVD's binding specificity to EpCAM-expressing cells was performed using a saturation test. To saturate EpCAM binding sites, a 100-fold (200 nM) excess of unlabeled DARPin Ec1 was added to a group of three cell-seeded dishes. An equal volume of media only was added to the second group of three cell-seeded dishes. The cells were incubated for 30 min at room temperature, thereafter radiolabeled EVD was added to obtain a final concentration of 2 nM. The cells were then incubated for 6 h at room temperature, and afterwards the medium was collected. The cells were washed and detached from the dishes by incubation with trypsin. The cell suspension was collected, and the activity of both the cells and media was measured to calculate the percentage of cell-bound activity. The unpaired two-tailed t-test was used to determine if a significant difference ($P<0.05$) between binding to pre-saturated and unsaturated cells existed.

To evaluate the internalization of Ec1 by renal carcinoma cells, ^{99m}Tc-EVD (which contained a residualizing label) was used. The internalization of ^{99m}Tc-EVD was studied during continuous incubation using the acid-wash method (30).

Radiolabeled ^{99m}Tc-EVD was added to the cells to obtain a concentration of 2 nM. The cells were incubated a 37˚C. After 1, 2, 4, 6 and 24 h of incubation, the media from the plated cells was collected. The cells were additionally washed once with fresh media. To collect the membrane-bound fraction, the cells were treated with a 0.2 M glycine buffer containing 4 M urea at pH 2.0 (which was placed on ice for 5 min before use) which caused dissociation of membrane-bound proteins. Afterwards, the cells were washed and treated with 1 M NaOH for 30 min in order to collect the fraction containing any internalized compound. The activity in every fraction was measured. The maximum value of cell-bound activity in each dataset was taken as 100% and the data were normalized to that value.

Affinity measurements using a LigandTracer. Binding affinities of the radiolabeled EVD to living SK-RC-52 renal carcinoma cells were measured using the LigandTracer instrument (Ridgeview Instruments). The TraceDrawer Software (Ridgeview Instruments AB) was used for evaluating the kinetics (31). The binding and dissociation kinetics were measured at room temperature. After a background measurement, increasing concentrations of radiolabeled EVD (1.8 and 5.4 nM) were added to the cells to determine the binding kinetics. After the association phase, the cell media was replaced and the retention in the dissociation phase was measured. The real time association and dissociation data were fitted into a one-to-one Langmuir binding model using the TraceDrawer Software. Both association and dissociation rates were determined, and the equilibrium dissociation constant was calculated.

Animal studies. Animal studies were performed according to national legislation on laboratory animal protection. The animal welfare was ensured by following The Guide for Care and Use of Laboratory Animals (32). After tumor implantation, the tumor size and animal behavior was monitored twice a week. To develop RCC xenografts, SK-RC-52 cells (10^7 cells in 100 μl media) were subcutaneously inoculated into the hind legs of female Balb/c nu/nu mice. The experiments were performed two weeks after SK-RC-52 cells implantation. At the time of experiment, the average mouse's weight was 18±2 g. The average tumor weight was 0.2±0.1 g (the largest tumor volume was 0.28 cm^3). A group of four animals point was used.

The biodistribution was measured using a dual-label technique. A mixture of both ^{125}I-EVD (20 kBq/mouse) and ^{99m}Tc-EVD (30 kBq/mouse) with a combined mass of 4 μg/mouse was injected as a solution in 100 μl PBS into the tail vein of mice. The biodistribution was measured 3 h post-injection. All animals were sedated by an intraperitoneal injection of a lethal dose of anesthesia (ketamine [Ketalar, Pfizer], 200 mg/kg of body weight, and xylazin [Rompun], 20 mg/kg of body weight). The sufficient degree of sedation was evaluated by absence of the pedal withdrawal reflex to toe pinch. The sedated animals were euthanized by a heart puncture with following exsanguination. The organs and tissues were collected, weighed and their activities were measured. The activity of iodine-125 in each sample was measured in the energy range between 18 and 85 keV. The activity of technetium-99m was measured in the energy range between 110 and 160 keV. These data were then used to calculate the percent of labelled compound taken up per gram of sample relative to the injected dose (%ID/g).

To test the specificity of EpCAM targeting *in vivo*, the uptake of tracers in EpCAM-positive SK-RC-52 tumors was compared to their uptake in EpCAM-negative xenografts produced using the Ramos lymphoma cell line (American Type Culture Collection). Lymphoma is an ideal negative control because it, unlike malignancies of epithelial origin, does not express EpCAM. On the other hand, Ramos lymphoma forms vascularized solid xenografts and might reflect nonspecific tumor accumulation *in vivo*. Ramos cells (10^7 cells) were subcutaneously inoculated into the hind legs of another group of female Balb/c nu/nu mice. The experiment was performed three weeks after Ramos cells implantation. At the time of experiment, the average mouse's weight was 18±2 g. The average tumor weight was 0.5±0.3 g (the largest tumor volume was 0.803 cm^3). A group of five animals was used. The injected activity and protein mass were the same as that used for mice bearing SK-RC-52 xenografts. The animals were euthanized after sedation (as aforementioned) by a heart puncture with subsequent exsanguination 3 h after injection, the xenografts were excised, and the uptake of the tracers was measured.

SPECT/CT scans of mice (bearing SK-RC-52 xenografts) injected with ^{99m}Tc-EVD (4 μg, 4.9 MBq) or with ^{125}I-EVD (4 μg, 2.5 MBq) in 100 μl PBS were performed using a nanoScan SPECT/CT platform (Mediso Medical Imaging Systems). The tumors size was 1.3x0.6 and 0.9x0.7 cm for animals imaged using ^{99m}Tc-EVD and ^{125}I-EVD, respectively. Imaging was performed 3 h post-injection. Immediately before imaging, the animals were euthanized by CO_2 asphyxiation (displacement rate 35% per minute), which caused them to urinate. In this way, the high activity from the urinary bladder is eliminated, which is a frequent artifact in preclinical studies. The animals' death was verified by lack of respiration and heartbeat and lack of response to toe pinch. The animals were positioned in the camera in a prone position, and imaging was performed using the protocol described in (28). The scanning time was 30 min.

Statistical analysis. The data are presented as the mean ± standard deviation of three samples for cell studies or four samples for animal studies. Data analyses for *in vitro* experiments were performed using an unpaired two-tailed t-test, the statistical significance threshold was set at P<0.05. The biodistribution data for the dual-label experiment were also analyzed using a paired two-tailed t-test, the statistical significance threshold was also set at P<0.05. The statistical analyses were performed using GraphPad Prism (version 7.02; GraphPad Software, Inc.).

Results

Radiolabeling. EVD was labelled with [^{99m}Tc][$Tc(CO)_3(H_2O)_3$]$^+$ using a triple histidine-glutamate tag, $(HE)_3$-tag, as a chelator to provide a residualizing label with a radiochemical yield of 58±16% (n=3). Labeling of EVD with the para-[^{125}I] iodobenzoyl group was performed by conjugating it as the N-hydroxysuccinimide ester (N-succinimidyl-para-[^{125}I] iodobenzoate) to the amino acid groups of lysine with a radiochemical yield of 16±3% (n=4). Purification using size-exclusion NAP-5 columns provided purities over 98% for both compounds.

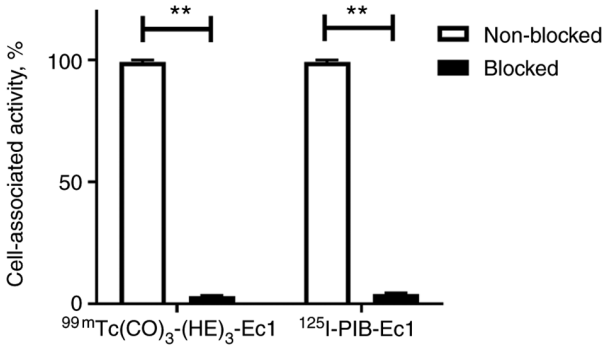

Figure 1. Binding specificity of ^{99m}Tc-EVD and ^{125}I-EVD to renal carcinoma cells. Data are normalized to specific binding of each conjugate. Error bars indicate the standard deviation. **P<0.005 vs. blocked control (unpaired t-test). EVD, epithelial cell adhesion molecule-visualizing designed ankyrin repeat protein.

Binding to RCC cells in vitro. For the specificity test, cells of the human carcinoma cell line SK-RC-52 were incubated with 2 nM of either ^{99m}Tc-EVD or ^{125}I-EVD, and the cell-associated activity was measured. In the control group, the binding sites of EpCAM were saturated by incubating cells in a 100-fold molar excess of unlabeled Ec1.

The blocking test showed that the pre-treatment of SK-RC-52 renal carcinoma cells with a large excess of unlabeled Ec1 resulted in a highly significant (P<0.00005) reduction in binding for both radiolabeled DARPins (Fig. 1).

According to sensorgrams from the LigandTracer instrument (Fig. 2), the binding of ^{99m}Tc-EVD to EpCAM-expressing renal carcinoma cells was rapid and showed an association rate constant or k_a value of $2.7(\pm0.2)x10^4$ $M^{-1}.s^{-1}$. Its dissociation was slow and showed a dissociation rate constant or k_d value of $1.1(\pm0.1)x10^{-5}$ s^{-1}. This resulted in a subnanomolar affinity or K_D value of 400±28 pM.

Internalization of ^{99m}Tc-EVD, after binding to renal carcinoma cells, was evaluated using the acid wash method. The data were normalized to the maximum value of cell-bound activity, and the cellular processing data are presented in Fig. 3. The total cell-associated and internalized activity increased continuously for the ^{99m}Tc-labeled variant. The internalization of ^{99m}Tc-EVD was slow, and only 20% was internalized after 24 h of incubation.

In vivo studies. The biodistribution evaluation of ^{125}I-EVD and ^{99m}Tc-EVD was measured in Balb/c nu/nu mice bearing SK-RC-52 renal carcinoma xenografts 3 h post-injection (pi). These data are presented in Figs. 4 and 5. Rapid blood clearance was observed for both radiolabeled-EVD variants. The tumor uptake of ^{125}I-EVD and ^{99m}Tc-EVD did not differ significantly. However, there were significant differences (P<0.05) in their distribution in normal tissues. The renal uptake of ^{99m}Tc-EVD was much higher than the renal uptake of its radioiodinated counterpart. Overall, ^{99m}Tc-EVD resulted in a significantly lower uptake in the blood, but ^{125}I-EVD provided a significantly lower uptake in the salivary glands, liver, spleen, stomach, kidneys and bones.

Based on these biodistribution features, ^{125}I-EVD provided significantly higher tumor-to-salivary gland, tumor-to-liver, tumor-to-spleen and tumor-to-kidney ratios compared to

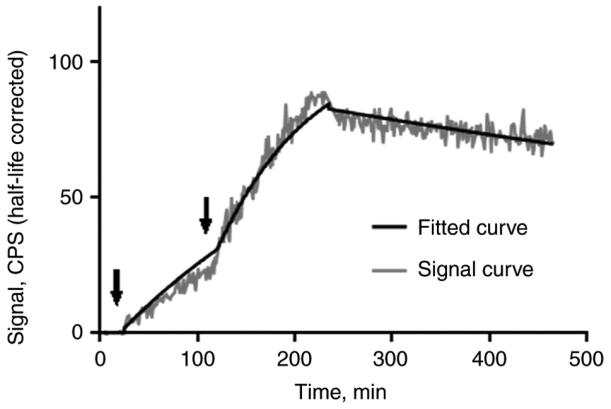

Figure 2. Representative ligand tracer sensorgram of ^{99m}Tc-epithelial cell adhesion molecule-visualizing designed ankyrin repeat protein binding to renal carcinoma cells. The first arrow indicates the moment of addition of the first concentration of the radiolabelled designed ankyrin repeat protein (1.8 nM), and the second arrow indicates the addition of the second concentration (5.4 nM). Cell-bound activity is presented as CPS. CPS, counts per sec.

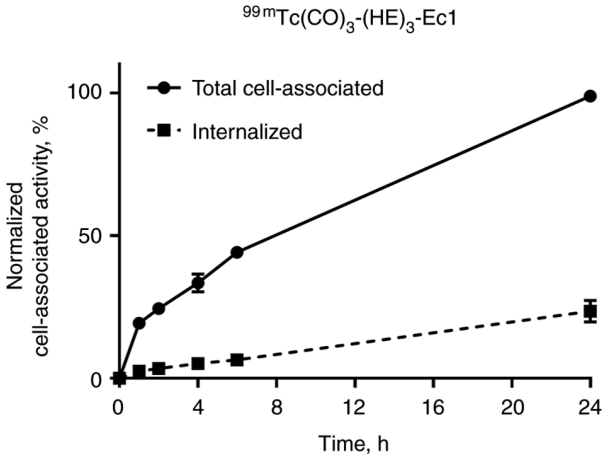

Figure 3. Cellular processing of ^{99m}Tc-epithelial cell adhesion molecule-visualizing designed ankyrin repeat protein by renal carcinoma cells during continuous incubation. Error bars indicate the standard deviation. Error bars may not be visible because they are smaller than the data point symbols.

^{99m}Tc-EVD (Fig. 5). However, ^{99m}Tc-EVD provided a higher tumor-to-blood ratio.

The uptake of both ^{125}I-EVD and ^{99m}Tc-EVD in EpCAM-negative Ramos lymphoma xenografts was significantly lower ($P<0.0001$) than in EpCAM-expressing SK-RC-52 xenografts (Fig. 6). This suggests that the recognition of EpCAM is a prerequisite for the accumulation of both tracers in tumors, i.e., the uptake is EpCAM-specific.

SPECT/CT imaging confirmed the findings of direct *ex vivo* measurements (Fig. 7). Both ^{99m}Tc-EVD and ^{125}I-EVD provided a clear visualization of SK-RC-52 renal carcinoma xenografts. Although there was some background activity in the whole body, in the case of ^{125}I-EVD, the contrast of the tumor visualization was high. It has to be noted that some spots with elevated activity accumulation (hot spots) were visible in the left femoral muscle of the mouse injected with ^{125}I-EVD. Most likely, these hot spots are reconstruction artefacts, as the image obtained using radioiodinated tracer is more pixelated. Most importantly, ^{125}I-EVD provided a much higher tumor contrast with respect to the kidneys and liver, which are the major metastatic sites for renal cell carcinoma. Overall, ^{125}I-EVD was the better probe for imaging EpCAM-expressing renal cell carcinomas.

Discussion

The overexpression of EpCAM, in an appreciable proportion of RCC cases (including the most frequent clear cell and papillary histological subtypes), makes it an attractive molecular target for the treatment of this disease. Still, a large number of patients have RCC tumors without sufficiently high levels of EpCAM expression for targeted therapy. This necessitates the stratification of patients for targeted anti-EpCAM treatment. Radionuclide-based molecular imaging would potentially enable a non-invasive analysis of EpCAM-expression levels in disseminated RCC cases.

Single-photon emission computed tomography (SPECT) offers the advantage of easy access around the world. Unlike positron emission tomography (PET), it is relatively available at hospitals in Africa, South America and Asia, where PET centers are not so common. Thus, the development of a SPECT-compatible imaging probe might have a greater impact on global healthcare.

The most suitable nuclides for SPECT imaging are technetium-99m ($T_{1/2}$=6 h, E_g=140 keV) and iodine-123 ($T_{1/2}$=13.3 h, E=159 keV). The energy of the gamma-ray photons from these nuclides provides an optimal combination of spatial resolution and photopeak registration efficiency for modern gamma-cameras. An additional advantage of technetium-99m is its production using the ^{99}Mo/^{99m}Tc-generator, which makes it cheaper and more readily available. However, the main criterion for suitability of an imaging probe is the sensitivity of imaging that it provides. The sensitivity depends on the imaging contrast, which is determined by the tumor-to-background uptake ratios for the main metastatic sites. The partial volume effect (which complicates visualization of small metastases) can be reduced with high tumor-to-background ratios.

Common metastatic sites for RCC include the lung (in 50-60 percent of metastatic cases), bone (in 30-40 percent), liver (in 30-40 percent) and brain (in 5 percent) (33). Accordingly, the most suitable tracer for imaging EpCAM in disseminated RCC should provide high tumor-to-lung, tumor-to-bone and tumor-to-liver uptake ratios. The tumor-to-brain ratio is less important because the brain uptake is generally very low for protein-based imaging probes when the blood-brain barrier is still intact. The judicious selection of a labelling strategy (i.e., a radionuclide, a chelator or linker for its coupling and the position of radionuclide coupling), which provides the lowest uptake in the aforementioned organs, would ensure the highest tumor-to-organ ratios and therefore result in the highest imaging sensitivity.

The fact that the selected labeling strategy determines the biodistribution of radiolabeled scaffold proteins is well established (25,34). For example, it has been demonstrated that an increase in negative charges on the N-terminus of affibody molecules (by selecting an appropriate combination of chelator and radionuclide) reduces their hepatic uptake (35).

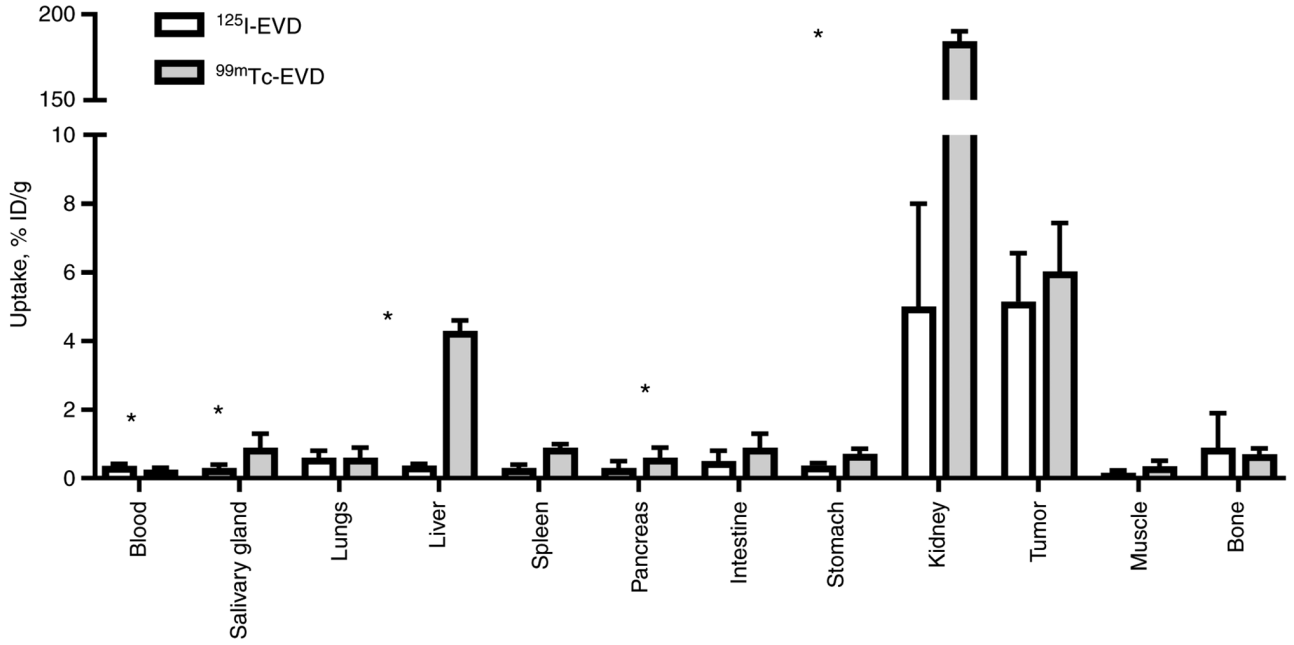

Figure 4. Comparative biodistribution of ^{99m}Tc-EVD and ^{125}I-EVD at 3 h post-injection in mice bearing renal carcinoma xenografts. Data are presented as percent ID per gram. Error bars indicate the standard deviation. *P<0.05, ^{99m}Tc-EVD vs. ^{125}I-EVD (paired t-test). EVD, epithelial cell adhesion molecule-visualizing designed ankyrin repeat protein; ID, injected dose.

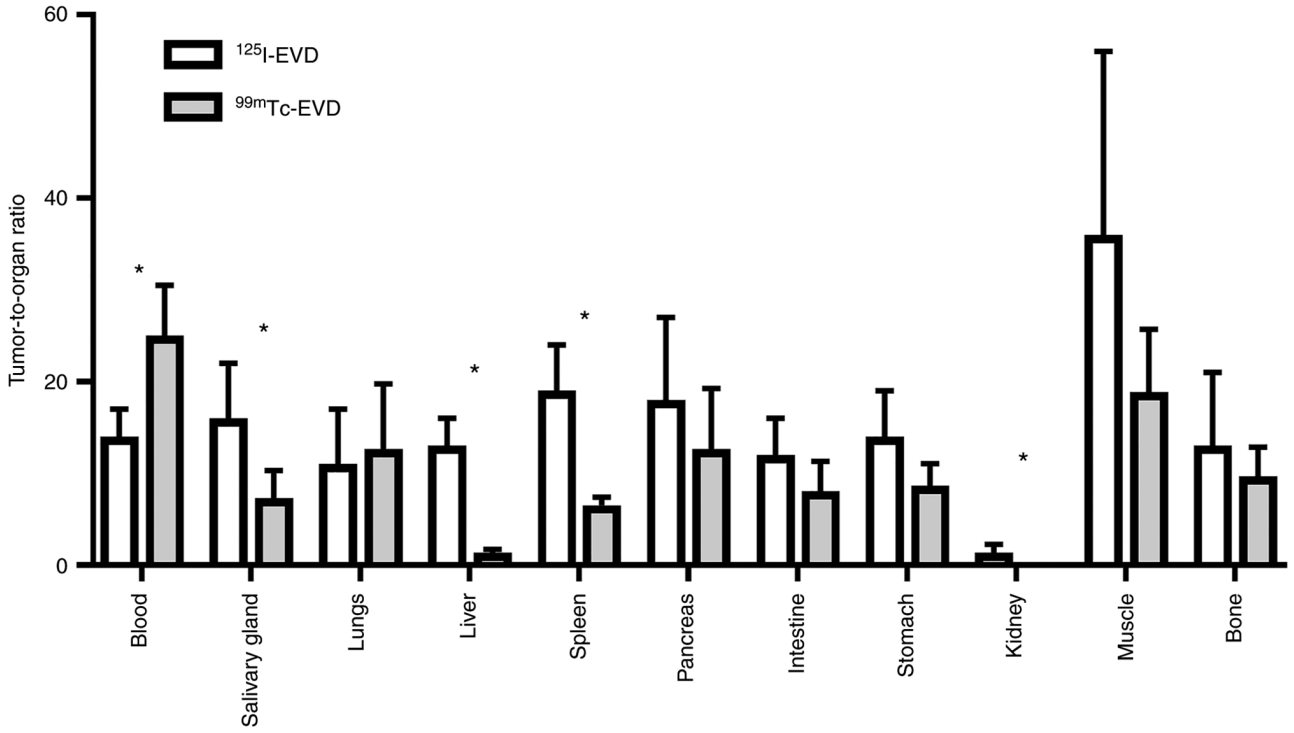

Figure 5. Comparison of tumor-to-organ ratios for ^{99m}Tc-EVD and ^{125}I-EVD at 3 h post-injection in mice bearing renal carcinoma xenografts. Error bars indicate the standard deviation. *P<0.05, ^{99m}Tc-EVD vs. ^{125}I-EVD (paired t-test). EVD, epithelial cell adhesion molecule-visualizing designed ankyrin repeat protein.

It has also been found that by using the negatively charged $(HE)_3$-tag as a chelator for $[^{99m}Tc][Tc(CO)_3(H_2O)_3]^+$ at the N-terminus of DARPins G3 (36) or Ec1 (29), a significant decrease of activity accumulation in the liver was observed. Results of previous studies (36,37) suggest that the uptake of DARPins in liver is not target-specific, but depends on unspecific interaction of protein-surface amino acids and a chelator with hepatocytes. In this case, it cannot be suppressed without re-engineering of the DARPins. Considering the importance of detecting hepatic metastases in RCC, the use of $(HE)_3$-tag as a chelator was selected for the ^{99m}Tc-labelling of EVD in this study.

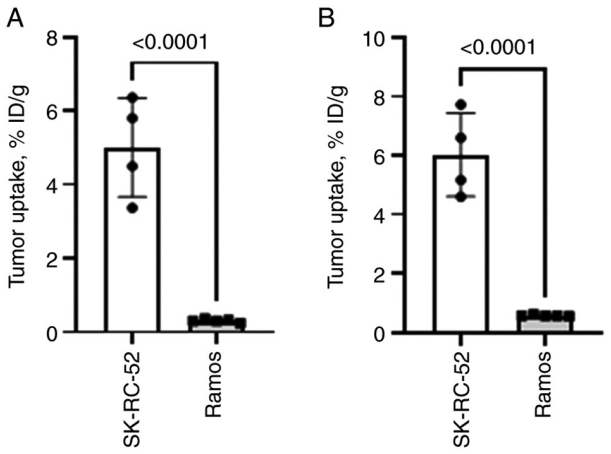

Figure 6. Specificity of EpCAM targeting *in vivo*. Comparison of (A) ^{125}I-EVD and (B) ^{99m}Tc-EVD in EpCAM-expressing SK-RC-52 renal carcinoma and EpCAM-negative Ramos lymphoma xenografts. Data are presented as percent ID per gram. Error bars indicate the standard deviation. P-values (unpaired t-test) are provided. EpCAM, epithelial cell adhesion molecule; EVD, epithelial cell adhesion molecule-visualizing designed ankyrin repeat protein; ID, injected dose.

An alternative strategy, which was also utilized in this study, is based on the use of non-residualizing labels, i.e., combinations of a nuclide and a chelator or a linker, which can diffuse through lysosomal and cytoplasmic membranes after internalization and lysosomal degradation of the targeting protein. Usually, such properties are demonstrated when proteins have been labelled with bromine-76, iodine-123, iodine-124, iodine-125 or iodine-131, because proteolysis of such proteins results in lipophilic radiometabolites capable of diffusing through membranes. It is essential when using this approach, that a targeted protein is internalized rapidly by excretory organs (e.g., liver and kidneys) but slowly by cancer cells. To test this approach in the current study, we evaluated radioiodinated Ec1. We have used the radionuclide iodine-125 ($T_{1/2}$=59.4 d) as a surrogate for iodine-123. These nuclides are identical from both a chemical and biochemical point of view, but the longer half-life and lower-energy electromagnetic radiation of iodine-125 make it more convenient for development work. It should also be noted that while leakage from excretory organs is a common feature of non-residualizing radioiodine labels, when coupled to scaffold proteins their influence on biodistribution is different. For example, the use of [(4-hydroxyphenyl)-ethyl] maleimide (HPEM) as a prosthetic group, for the radioiodination of both anti-HER2 DARPin G3 and anti-EpCAM DARPin Ec1, resulted in a massive hepatobiliary excretion and accumulation of activity in the gastrointestinal tract (37,38). Since excess activity in the gastrointestinal tract would complicate the imaging of abdominal metastases in RCC, this method was excluded from the current study.

One particular approach to radioiodination includes so-called direct radioiodination, i.e., when an *in-situ* oxidized radioiodine attacks the tyrosine residues of a protein. The main radiometabolite of directly-iodinated proteins is radioiodotyrosine, which has typical non-residualizing properties. An advantage of direct radioiodination is usually the high labelling yield. Although there is a risk that iodination of tyrosines might reduce the binding strength of scaffold proteins (39), directly-radioiodinated DARPins have been shown to preserve their binding capacity (29,40). An alternative method to radioiodination is an indirect approach by conjugating a radioiodobenzoyl (e.g., PIB) group. The yield of such labeling is typically lower than the yield of direct radioiodination. However, an advantage of this labeling approach is the rapid excretion of radiometabolites from the blood without accumulation in any other organ or tissue. A comparison between directly and indirectly radioiodinated DARPins G3 and Ec1, has shown that the redistribution of radiometabolites from the directly iodinated variants resulted in appreciably elevated activity uptake in the blood, organs expressing the Na/I-symporter and a number of other tissues (including the gastrointestinal tract). However, the indirectly iodinated variants (using radioactive-PIB) demonstrated appreciably lower activity uptake in these organs and higher tumor-to-organ ratios in the abdomen (29,41). Therefore, indirect radioiodination using [^{125}I]PIB was selected for the imaging of EpCAM expression in RCC.

The labeling procedures for both ^{99m}Tc-EVD and ^{125}I-EVD provided conjugates with radiochemical purity over 98%, which makes their clinical application possible. The binding of both conjugates to EpCAM-expressing renal carcinoma cells was significantly reduced by pre-saturating the EpCAM-binding sites. This demonstrated that neither labeling procedure compromised the EpCAM-specific binding character of the targeting protein. In order to evaluate the internalization rate by RCC cells, we used ^{99m}Tc-EVD with its residualizing label. If the non-residualizing radioiodine label was used instead, it would have resulted in leakage of radiometabolites from the cells and an underestimation of the internalized activity. The internalized activity was found to be below 15% of the total cell-bound activity after the first 6 h of incubation, i.e., the internalization of ^{99m}Tc-EVD by RCC cells was slow. Because of this slow internalization, the retention of activity in tumors *in vivo* should not be affected by the residualizing properties of the label, but rather, it should mainly depend on the strength of the tracers' binding to their molecular target (located on the membranes of malignant cells). The binding affinity of radiolabeled Ec1 to SK-RC-52 renal carcinoma cells was very high, 400±28 pM, which is a prerequisite for successful targeting (with both ^{99m}Tc-EVD and ^{125}I-EVD) to be achieved.

The results from the biodistribution experiments confirmed equal targeting efficiency for both ^{99m}Tc-EVD and ^{125}I-EVD. The tumor uptake of both tracers did not differ significantly at 3 h after injection (5.2±1.4%ID/g for ^{125}I-EVD vs. 6.0±1.4%ID/g for ^{99m}Tc-EVD). Importantly, the accumulation of both tracers in the SK-RC-52 xenografts was EpCAM-dependent. However, the main difference observed was between the uptakes of tracers in normal tissues. The blood-born activity was low, but the concentration was significantly higher ($P<0.05$) for ^{125}I-EVD (0.37±0.06%ID/g) than it was for ^{99m}Tc-EVD (0.25±0.06%ID/g). This difference is most likely due to the retention pattern of radiometabolites in the kidneys. Previous studies demonstrated that DARPins clear rapidly form blood via kidneys, but they are reabsorbed in proximal tubules after glomerular filtration. This reabsorption cannot be blocked with a co-infusion of lysine or Gelofusine (42), which blocks sometimes for other radiolabeled proteins or peptides. In the case of a residualizing label,

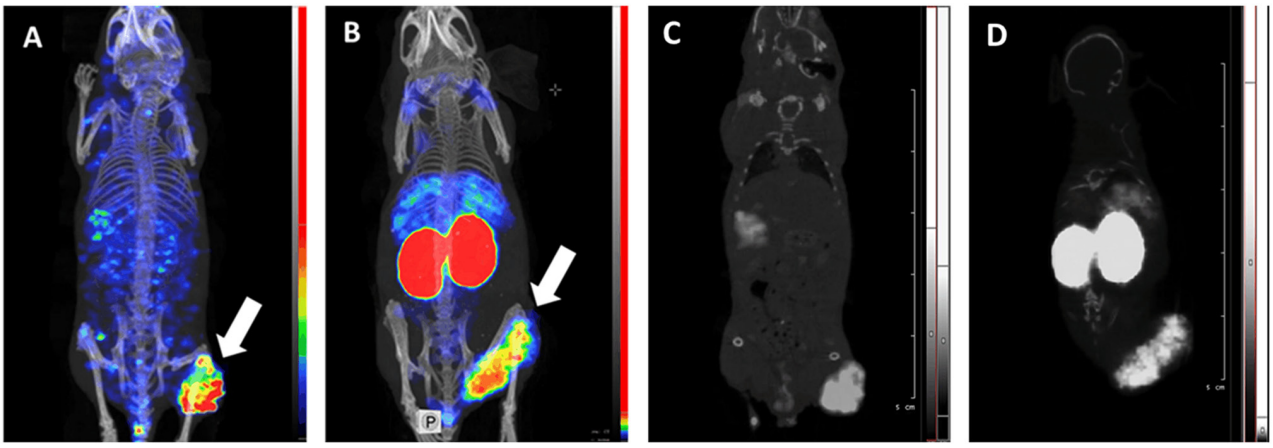

Figure 7. Micro-single photon emission CT/CT imaging using (A and C) ^{125}I-EVD and (B and D) ^{99m}Tc-EVD at 3 h post-injection. Images show (A and B) maximum intensity projections and (C and D) coronal sections. Arrows point at tumors. P, posterior image.

this phenomenon results in high renal uptake of activity after injection of anti-HER2 or anti-EpCAM DARPins labeled with residualizing radiometals (28,36,38). In this study, metabolites from the residualizing [^{99m}Tc][Tc(CO)$_3$]$^+$ label remained in the kidneys after reabsorption and degradation (the renal uptake was 184±6%ID/g) while the metabolites of the [^{125}I]PIB label left the kidneys (the renal uptake was 5±1%ID/g). It is conceivable that a part of the renal metabolites from the [^{125}I]PIB label appears in the blood and contributes to the total activity concentration in the blood. The difference in radiometabolite retention is the most plausible cause of the significantly higher ($P<0.05$) technetium-99m activity in the salivary gland, liver, spleen and intestines. This difference in the biodistribution is linked with the significantly higher ($P<0.05$) tumor-to-salivary gland, tumor-to-liver, tumor-to-spleen and tumor-to-intestinal wall ratios for ^{125}I-EVD. These findings were confirmed by experimental microSPECT imaging. The apparent higher imaging contrast for tumors in abdominal tissues makes ^{125}I-EVD a better imaging probe for visualizing EpCAM expression in metastases of renal cell carcinoma and for selecting patients for EpCAM-targeted therapy.

In conclusion, the low retention of ^{125}I-EVD radiometabolites in normal tissues ensures high tumor-to-organ uptake ratios and results in a high imaging contrast for the visualization of metastases of RCC. Radioiodinated DARPin Ec1 is the most suitable imaging agent for the selection of RCC patients for EpCAM-targeted therapy.

Acknowledgements

The authors would like to thank Mr. Tyran Günther (Department of Materials Science and Engineering, Uppsala University, Uppsala, Sweden) for proofreading the manuscript.

Funding

This research was funded by grants from the Swedish Cancer Society Cancerfonden (20 0181; 20 0893 Pj; 21 1485 Pj), Ministry of Science and Higher Education RF (075-15-2022-1103) and Swedish Research Council Vetenskapsrådet (VR 2019-00994).

Availability of data and materials

The datasets used and/or analyzed during the current study are available from the corresponding author on reasonable request.

Authors' contributions

VT, VB, AO and AV performed the experiments and analyzed the data. AS and SMD performed the production and purification of proteins. SMD participated in the molecular design, supervised the production, purification and characterization of protein, and coordinated the work. AV obtained funding, participated in the study design, labelling chemistry development, data treatment and interpretation, and coordinated the work. VT obtained funding, and participated in the study design, data treatment and interpretation. VT and VB wrote the first version of the manuscript. AV and VT confirm the authenticity of all the raw data. All authors have agreed to be held accountable for all aspects of the research, including the accuracy and integrity of all parts of the work. All authors read and approved the final manuscript.

Ethics approval and consent to participate

Animal studies were approved by the local ethics committee for animal research in Uppsala (Uppsala djurförsöksetiska nämnd), Sweden (ethical permission C5/16 from 26-02-2016).

Patient consent for publication

Not applicable.

Competing interests

The authors declare that they have no competing interests.

References

1. Ljungberg B, Bensalah K, Canfield S, Dabestani S, Hofmann F, Hora M, Kuczyk MA, Lam T, Marconi L, Merseburger AS, *et al*: EAU guidelines on renal cell carcinoma: 2014 update. Eur Urol 67: 913-924, 2015.

2. Ryan CW, Vogelzang NJ and Stadler WM: A phase II trial of intravenous gemcitabine and 5-fluorouracil with subcutaneous interleukin-2 and interferon-alpha in patients with metastatic renal cell carcinoma. Cancer 94: 2602-2609, 2002.
3. Went P, Dirnhofer S, Salvisberg T, Amin MB, Lim SD, Diener PA and Moch H: Expression of epithelial cell adhesion molecule (EpCam) in renal epithelial tumors. Am J Surg Pathol 29: 83-88, 2005.
4. Stewart GD, O'Mahony FC, Powles T, Riddick AC, Harrison DJ and Faratian D: What can molecular pathology contribute to the management of renal cell carcinoma? Nat Rev Urol 8: 255-265, 2011.
5. Tran J and Ornstein MC: Clinical review on the management of metastatic renal cell carcinoma. JCO Oncol Pract 18: 187-196, 2022.
6. Osawa T, Takeuchi A, Kojima T, Shinohara N, Eto M and Nishiyama H: Overview of current and future systemic therapy for metastatic renal cell carcinoma. Jpn J Clin Oncol 49: 395-403, 2019.
7. Tung I and Sahu A: Immune checkpoint inhibitor in first-line treatment of metastatic renal cell carcinoma: A review of current evidence and future directions. Front Oncol 11: 707214, 2021.
8. Elias DJ, Kline LE, Robbins BA, Johnson HC Jr, Pekny K, Benz M, Robb JA, Walker LE, Kosty M and Dillman RO: Monoclonal antibody KS1/4-methotrexate immunoconjugate studies in non-small cell lung carcinoma. Am J Respir Crit Care Med 150: 1114-1122, 1994.
9. Braun S, Hepp F, Kentenich CR, Janni W, Pantel K, Riethmüller G, Willgeroth F and Sommer HL: Monoclonal antibody therapy with edrecolomab in breast cancer patients: Monitoring of elimination of disseminated cytokeratin-positive tumor cells in bone marrow. Clin Cancer Res 5: 3999-4004, 1999.
10. Punt CJ, Nagy A, Douillard JY, Figer A, Skovsgaard T, Monson J, Barone C, Fountzilas G, Riess H, Moylan E, *et al*: Edrecolomab alone or in combination with fluorouracil and folinic acid in the adjuvant treatment of stage III colon cancer: A randomised study. Lancet 360: 671-677, 2002.
11. Di Paolo C, Willuda J, Kubetzko S, Lauffer I, Tschudi D, Waibel R, Plückthun A, Stahel RA and Zangemeister-Wittke U: A recombinant immunotoxin derived from a humanized epithelial cell adhesion molecule-specific single-chain antibody fragment has potent and selective antitumor activity. Clin Cancer Res 9: 2837-2848, 2003.
12. Andersson Y, Inderberg EM, Kvalheim G, Herud TM, Engebraaten O, Flatmark K, Dueland S and Fodstad Ø: Immune stimulatory effect of anti-EpCAM immunotoxin-improved overall survival of metastatic colorectal cancer patients. Acta Oncol 59: 404-409, 2020.
13. Seimetz D, Lindhofer H and Bokemeyer C: Development and approval of the trifunctional antibody catumaxomab (anti-EpCAM x anti-CD3) as a targeted cancer immunotherapy. Cancer Treat Rev 36: 458-467, 2010.
14. Martin-Killias P, Stefan N, Rothschild S, Plückthun A and Zangemeister-Wittke U: A novel fusion toxin derived from an EpCAM-specific designed ankyrin repeat protein has potent antitumor activity. Clin Cancer Res 17: 100-110, 2011.
15. Xu T, Vorobyeva A, Schulga A, Konovalova E, Vorontsova O, Ding H, Gräslund T, Tashireva LA, Orlova A, Tolmachev V and Deyev SM: Imaging-Guided therapy simultaneously targeting HER2 and EpCAM with trastuzumab and EpCAM-Directed toxin provides additive effect in ovarian cancer model. Cancers (Basel) 13: 3939, 2021.
16. Zhang BL, Li D, Gong YL, Huang Y, Qin DY, Jiang L, Liang X, Yang X, Gou HF, Wang YS, *et al*: Preclinical evaluation of chimeric antigen receptor-modified T cells specific to epithelial cell adhesion molecule for treating colorectal cancer. Hum Gene Ther 30: 402-412, 2019.
17. Pilanc KN, Ordu Ç, Akpnar H, Balc C, Başsülü N, Köksal Üİ, Elbüken F, Okutur K, Bülbül G, Sağlam S and Demir G: Dramatic response to catumaxomab treatment for malign ascites related to renal cell carcinoma with sarcomotoid differentiation. Am J Ther 23: e1078-e1081, 2016.
18. Schmidt M, Scheulen ME, Dittrich C, Obrist P, Marschner N, Dirix L, Schmidt M, Rüttinger D, Schuler M, Reinhardt C and Awada A: An open-label, randomized phase II study of adecatumumab, a fully human anti-EpCAM antibody, as monotherapy in patients with metastatic breast cancer. Ann Oncol 21: 275-282, 2010.
19. Marschner N, Rüttinger D, Zugmaier G, Nemere G, Lehmann J, Obrist P, Baeuerle PA, Wolf A, Schmidt M, Abrahamsson PA, *et al*: Phase II study of the human anti-epithelial cell adhesion molecule antibody adecatumumab in prostate cancer patients with increasing serum levels of prostate-specific antigen after radical prostatectomy. Urol Int 85: 386-395, 2010.
20. Zimpfer A, Maruschke M, Rehn S, Kundt G, Litzenberger A, Dammert F, Zettl H, Stephan C, Hakenberg OW and Erbersdobler A: Prognostic and diagnostic implications of epithelial cell adhesion/activating molecule (EpCAM) expression in renal tumours: A retrospective clinicopathological study of 948 cases using tissue microarrays. BJU Int 114: 296-302, 2014.
21. Bensch F, Lamberts LE, Smeenk MM, Jorritsma-Smit A, Lub-de Hooge MN, Terwisscha van Scheltinga AGT, de Jong JR, Gietema JA, Schröder CP, Thomas M, *et al*: 89Zr-Lumretuzumab PET Imaging before and during HER3 antibody lumretuzumab treatment in patients with solid tumors. Clin Cancer Res 23: 6128-6137, 2017.
22. Jauw YW, Zijlstra JM, de Jong D, Vugts DJ, Zweegman S, Hoekstra OS, van Dongen GA and Huisman MC: Performance of 89Zr-Labeled-Rituximab-PET as an Imaging Biomarker to Assess CD20 Targeting: A pilot study in patients with relapsed/refractory diffuse large B cell lymphoma. PLoS One 12: e0169828, 2017.
23. Ulaner GA, Lyashchenko SK, Riedl C, Ruan S, Zanzonico PB, Lake D, Jhaveri K, Zeglis B, Lewis JS and O'Donoghue JA: First-in-Human human epidermal growth factor receptor 2-Targeted Imaging Using 89Zr-Pertuzumab PET/CT: Dosimetry and clinical application in patients with breast cancer. J Nucl Med 59: 900-906, 2018.
24. Garousi J, Orlova A, Frejd FY and Tolmachev V: Imaging using radiolabelled targeted proteins: Radioimmunodetection and beyond. EJNMMI Radiopharm Chem 5: 16, 2020.
25. Tolmachev VM, Chernov VI and Deyev SM: Targeted nuclear medicine. Seek and destroy. Rus Chem Rev 91: RCR5034, 2022.
26. Plückthun A: Designed ankyrin repeat proteins (DARPins): Binding proteins for research, diagnostics, and therapy. Annu Rev Pharmacol Toxicol 55: 489-511, 2015.
27. Stefan N, Martin-Killias P, Wyss-Stoeckle S, Honegger A, Zangemeister-Wittke U and Plückthun A: DARPins recognizing the tumor-associated antigen EpCAM selected by phage and ribosome display and engineered for multivalency. J Mol Biol 413: 826-843, 2011.
28. Deyev SM, Vorobyeva A, Schulga A, Abouzayed A, Günther T, Garousi J, Konovalova E, Ding H, Gräslund T, Orlova A and Tolmachev V: Effect of a radiolabel biochemical nature on tumor-targeting properties of EpCAM-binding engineered scaffold protein DARPin Ec1. Int J Biol Macromol 145: 216-225, 2020.
29. Vorobyeva A, Bezverkhniaia E, Konovalova E, Schulga A, Garousi J, Vorontsova O, Abouzayed A, Orlova A, Deyev S and Tolmachev V: Radionuclide molecular imaging of EpCAM expression in triple-negative breast cancer using the scaffold protein DARPin Ec1. Molecules 25: 4719, 2020.
30. Wållberg H and Orlova A: Slow internalization of anti-HER2 synthetic affibody monomer 111In-DOTA-ZHER2:342-pep2: Implications for development of labeled tracers. Cancer Biother Radiopharm 23: 435-442, 2008.
31. Tolmachev V, Orlova A and Andersson K: Methods for radiolabelling of monoclonal antibodies. Methods Mol Biol 1060: 309-330, 2014.
32. Guide for the Care and Use of Laboratory Animals. The National Academies Press, Washington, DC, 1996. https://doi.org/10.17226/5140.
33. Motzer RJ, Bander NH and Nanus DM: Renal-cell carcinoma. N Engl J Med 335: 865-875, 1996.
34. Tolmachev V and Orlova A: Affibody molecules as targeting vectors for PET Imaging. Cancers (Basel) 12: 651, 2020.
35. Hosseinimehr SJ, Tolmachev V and Orlova A: Liver uptake of radiolabeled targeting proteins and peptides: Considerations for targeting peptide conjugate design. Drug Discov Today 17: 1224-1232, 2012.
36. Vorobyeva A, Schulga A, Konovalova E, Güler R, Löfblom J, Sandström M, Garousi J, Chernov V, Bragina O, Orlova A, *et al*: Optimal composition and position of histidine-containing tags improves biodistribution of ^{99m}Tc-labeled DARPin G3. Sci Rep 9: 9405, 2019.
37. Deyev SM, Xu T, Liu Y, Schulga A, Konovalova E, Garousi J, Rinne SS, Larkina M, Ding H, Gräslund T, *et al*: Influence of the position and composition of radiometals and radioiodine labels on imaging of Epcam expression in prostate cancer model using the DARPin Ec1. Cancers (Basel) 13: 3589, 2021.
38. Vorobyeva A, Schulga A, Konovalova E, Güler R, Mitran B, Garousi J, Rinne S, Löfblom J, Orlova A, Deyev S and Tolmachev V: Comparison of tumor-targeting properties of directly and indirectly radioiodinated designed ankyrin repeat protein (DARPin) G3 variants for molecular imaging of HER2. Int J Oncol 54: 1209-1220, 2019.

39. Wikman M, Steffen AC, Gunneriusson E, Tolmachev V, Adams GP, Carlsson J and Ståhl S: Selection and characterization of HER2/neu-binding affibody ligands. Protein Eng Des Sel 17: 455-462, 2004.
40. Deyev S, Vorobyeva A, Schulga A, Proshkina G, Güler R, Löfblom J, Mitran B, Garousi J, Altai M, Buijs J, *et al:* Comparative evaluation of Two DARPin variants: Effect of affinity, size, and label on tumor targeting properties. Mol Pharm 16: 995-1008, 2019.
41. Vorobyeva A, Schulga A, Rinne SS, Günther T, Orlova A, Deyev S and Tolmachev V: Indirect radioiodination of DARPin G3 Using N-succinimidyl-Para-Iodobenzoate Improves the Contrast of HER2 molecular imaging. Int J Mol Sci 20: 3047, 2019.
42. Altai M, Garousi J, Rinne SS, Schulga A, Deyev S and Vorobyeva A: On the prevention of kidney uptake of radiolabeled DARPins. EJNMMI Res 10: 7, 2020.